Stacking Design in Inverse Perovskites: The System $(Sr_{3-x}Ba_xN)Bi$

Frank Gäbler, Miriam Schmidt, Helge Rosner, Gudrun Auffermann and Rainer Niewa [1]

The cubic Perovskite structure is one of the most stable atomic arrangements for ternary and multinary compounds and — together with its distortion variants — found for an overwhelming number of compounds. Additionally, with certain bonding or atomic radii constraints, so-called hexagonal Perovskites, stacking variants of the cubic Perovskite, are known, which constitute a large group of compounds with a multitude of interesting and useful properties. Inverse Perovskites result from interchange of crystallographic positions of anions by cations, and vice versa. Although examples for inverse Perovskites are known for more than 150 years, the number of normal Perovskites and hexagonal/trigonal stacking or distortion variants is unequalled. Until recently, only cubic inverse Perovskites, one distortion variant thereof and one example for a hexagonal Perovskite with 2H structure were known. The substitution series $(Sr_{3-x}Ba_xN)Bi$ is shown as an example how unprecedented inverse stacking variants can be obtained and rationally predicted.

Ternary nitrides of the general composition $(Ca_3N)E$ are known for a couple of years. The compounds crystallize in a cubic inverse Perovskite type crystal structure (E = Tl, Ge, Sn, Pb, Sb, Bi and Au) or in an orthorhombic distortion variant thereof (E = P, As) [1 – 4]. Recent reports deal with ternary nitrides of the composition $(A_3N_x)E$ with A = Ba, Sr and E = Sn, Pb ($0.66 \leq x \leq 0.82$), Sb, Bi (x = 1) [5, 6]. The compounds of the composition $(Ba_3N_x)E$ and $(Sr_3N_x)E$ (E = Sn, Pb) crystallize in a cubic inverse Perovskite type structure with a nitride deficiency and show metallic properties. The semiconducting compounds $(Sr_3N)E$ with E = Sb, Bi also crystallize in a cubic inverse Perovskite type structure (Fig. 1a), while the structures of $(Ba_3N)E$ correspond to inverse 2H-Perovskites ($BaNiO_3$-type, see Fig. 1d).

On substitution of strontium by barium within the cubic Perovskites $(Sr_3N)E$ (E = Sb, Bi), i. e., the quasibinary systems $(Sr_3N)E$–$(Ba_3N)E$, a structural change from the cubic to the hexagonal 2H-Perovskite conducts via a 4H variant and a 9R variant. While the cubic Perovskites can be described as consisting of a three-dimensional framework of vertex-linked A_6N-octahedra with E^{3-} ions in large cuboctahedrally coordinated voids (Fig. 1a), those octahedra are face-sharing in the 2H-Perovskite variant (Fig. 1d). This leads to infinite rods of face-sharing octahedra and anticuboctahedral coordination of E^{3-}. The hexagonal stacking variants 4H and 9R contain elements of the cubic as well as the hexagonal 2H-Perovskite variants. In the 4H structure blocks (Fig. 1b) two face-sharing octahedra are inter-linked via all six terminal corners to a three-dimensional framework, whereas in the 9R structure a framework of interconnected blocks of three face-sharing octahedra is found. In a different description based on stacking of hexagonal A_3Bi-layers the stacking sequence **...ABC...** corresponds to the cubic Perovskite, **…ABAC…** to the 4H structure, **…ABABCBCAC…** to the 9R variant, and **...AB...** to the 2H-Perovskite.

For the example of the system $(Ba_xSr_{3-x}N)Bi$ and a temperature of 1148 K the homogeneity ranges are as follows:

range of existence cubic Perovskite:
$0.00 \leq x \leq 0.90$
range of existence stacking variant 4H:
$1.55 \leq x \leq 2.10$
range of existence stacking variant 9R:
$2.50 \leq x \leq 2.55$
range of existence hexagonal Perovskite 2H:
$2.75 \leq x \leq 3.00$.

As one might expect, the homogeneity ranges are separated by two-phase ranges of various widths. These data are graphically presented in Fig. 2. Naturally, phases with significant homogeneity ranges exhibit defects, disorder, or, in the presented case, partial ordering of the two different alkaline-earth metal constituents. The mechanism of the transition from cubic Perovskite via the various hexagonal stacking variants on increasing barium content was studied with X-ray and neutron powder diffraction. Obtained compositions from the refinements for the different phases are in excellent agreement with results from full chemical analyses.

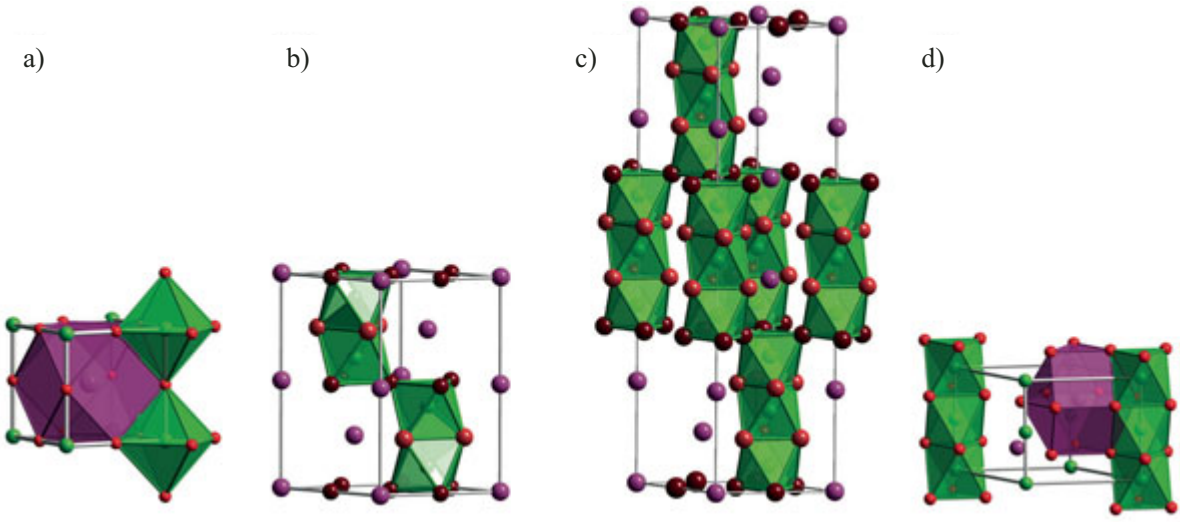

Fig. 1: Structure representations of compounds $(Sr_{3-x}Ba_xN)E$ (E = Sb, Bi) with a) a cubic Perovskite structure (x ≈ 0.0), b) a 4H $BaMnO_3$ type structure (x ≈ 2.0), c) a 9R $BaRuO_3$ type structure (x ≈ 2.5) and d) a 2H $BaNiO_3$ type structure (x ≈ 3.0, from left to right). Green spheres: N, violet spheres: E = Sb, Bi, dark red spheres: mainly Sr, light red spheres: mainly Ba. Sr is predominantly located at vertex-sharing sites of (A_6N) octahedral (green), Ba at face-sharing positions.

The order scheme of Sr and Ba on the different crystallographic sites, respectively their arrangement concerning the other involved constituents N^{3-} and Bi^{3-} gives hints for an understanding of the crystallographic relations. As can be taken from Fig. 2, within the homogeneity ranges of the phases the unit cell volumina increase linearly with increasing barium content and thus follow the rule of *Vegard*. While the cubic Perovskites are constraint to the ideal *c*/*a* ratio of a close packing, the 4H-, 9R- and the 2H-Perovskite show a deviation from the ideal *c*/*a* proportion to larger values. The reason is an increased repulsive N^{3-}–N^{3-} coulomb interaction in the hexagonal variants, because of shorter N–N distances as compared to the cubic Perovskite. The distortion increases with increasing number of face-sharing octahedra. This interaction is partially compensated by elongation of the octahedra in the [001] direction ($V \propto a^2c$: compression in *a* direction), partially by displacement of the nitride ions in the terminal octahedra of the blocks from the ideal position (4H and 9R).

On going from $(Sr_3N)Bi$ to $(Ba_3N)Bi$ the closed packing of Sr and Bi is expanded by substitution of strontium by barium. The resulting increased bonding distance *A*–N result in decreasing attractive coulomb interactions between Sr^{2+} and N^{3-}. A closer packing of *A* and Bi in a Ba-richer region is achieved by changes of the crystal structure from cubic to the stacking variants 4H-, 9R- and finally to the 2H-Perovskite. In the stacking variants 4H- and 9R this structural changes proceed with a concomitant partial ordering of Ba^{2+}/Sr^{2+} on the different crystallographic sites. As a general rule, A_6N octahedra are preferably inter-linked at vertex by Sr^{2+} ions and face-shared via Ba^{2+} ions. Within this ordering scheme attractive Sr^{2+}–N^{3-} and repulsive N^{3-}–N^{3-} coulomb interactions are adjusted in similar direction. A complete ordering of Ba^{2+}/Sr^{2+} is not achieved due to structural mismatch with a closed packing.

All phases containing group 15 elements, here specifically bismuth, can be rationalized exclusively containing closed shell particles according to $(A^{2+})_3N^{3-}Bi^{3-}$. Measurements of the electrical resistivity and the magnetic susceptibility reveal semiconducting and diamagnetic behavior, respectively.

In addition, the phase stability and the electronic properties of $(Ba_3N)E$ and $(Sr_3N)E$ (*E* = Sb, Bi) were investigated by *ab intio* electronic structure calculations. The calculations were done using the full potential minimal basis code FPLO [7]. At ambient conditions, the calculated ground state structures are in agreement with the experimental observations. Semiconducting behaviour was found for all compounds with band gaps between 0.15 eV and 0.5 eV (see fig.3).

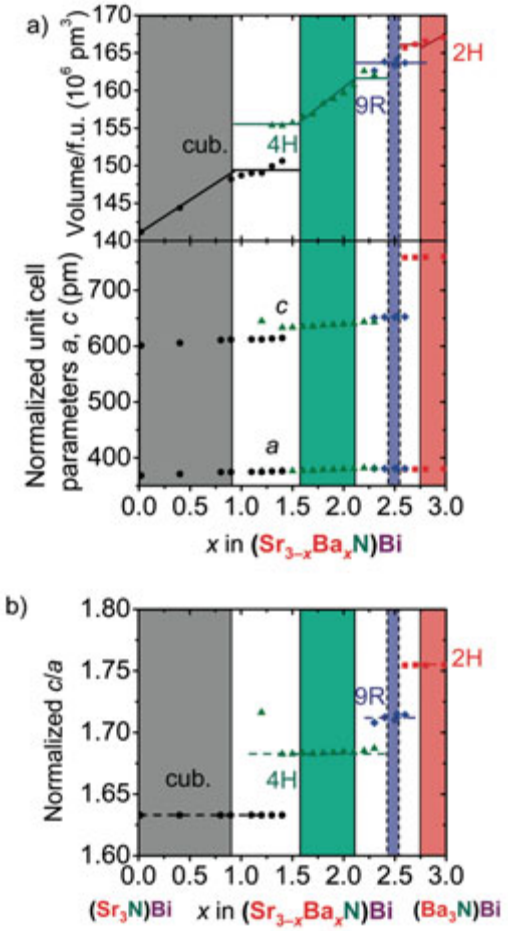

Fig. 2: Dependence of a) unit cell dimensions and volumes b) the normalized c/a ratio of phases $(Sr_{3-x}Ba_xN)Bi$ on x (open symbols: from experiments at T = 1070 K, full symbols: from experiments at T = 1120 K). The structural representations depict the stacking in the different polytypes.

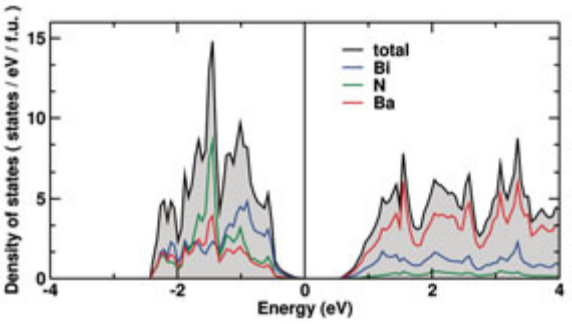

Fig. 3: Total and partial density of states of the hexagonal $(Ba_3N)Bi$ at normal conditions. Whereas the valence band states originate almost equally from Bi, Ba and N, the conduction band above the band gap is dominated by Ba states. The Fermi level is located at zero energy.

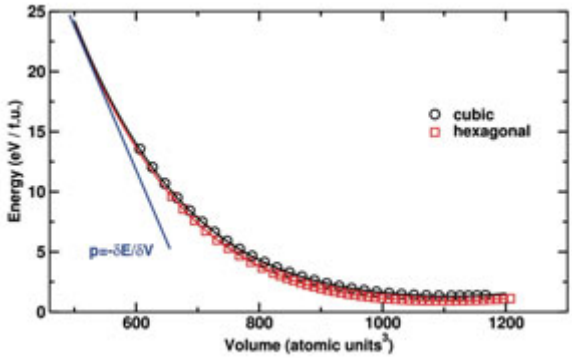

Fig. 4: Energy-versus-volume curve for $(Ba_3N)Bi$. At normal conditions, the hexagonal phase (2H, red squares) is lower in energy than the cubic phase (black circles). The transition pressure p can be estimated by the negative slope –δE/δV of the common tangent.

Because the application of "chemical pressure" due to the substitution of Sr by Ba leading to structural changes from the cubic to the hexagonal phase, the stability of the hexagonal Ba compounds with respect to external hydrostatic pressure was studied. Calculating the energy-versus-volume curves for $(Ba_3N)Bi$ and $(Ba_3N)Sb$, transition pressures of 129 GPa and 67 GPa from the hexagonal to the cubic phase were estimated (see Fig. 4). This transition is accompanied by an insulator–metal transition. The occurrence of other stacking variants below the above mentioned transition pressures is most likely and currently under investigation.

[1] Present address: TU München, München, Germany

References

[1] *R. Niewa, W. Schnelle and F. R. Wagner,* Z. Anorg. Allg. Chem. **627** (2001) 365.

[2] *M. Y. Chern, D. A. Vennos and F. J. DiSalvo,* J. Solid State Chem. **96** (1992) 415.

[3] *J. Jäger, D. Stahl, P. C. Schmidt and R. Kniep,* Angew. Chem. Int. Ed. **32** (1993) 709.

[4] *M. Y. Chern, F. J. DiSalvo, J. B. Parise and J. A. Goldstone*, J. Solid State Chem. **96** (1992) 426.

[5] *F. Gäbler, M. Kirchner, W. Schnelle, U. Schwarz, M. Schmitt*, *H. Rosner and R. Niewa,* Z. Anorg. Allg. Chem. **630** (2004) 2292.

[6] *F. Gäbler, M. Kirchner, W. Schnelle, M. Schmitt, H. Rosner and R. Niewa,* Z. Anorg. Allg. Chem. **631** (2004) 397.

[7] *K. Koepernik and H. Eschrig*, Phys. Rev. B **59** (1999) 1743.